



Swansea University
Prifysgol Abertawe



Cronfa - Swansea University Open Access Repository

This is an author produced version of a paper published in:

Geophysical Research Letters

Cronfa URL for this paper:

<http://cronfa.swan.ac.uk/Record/cronfa48822>

Paper:

Young, G., Gagen, M., Loader, N., McCarroll, D., Grudd, H., Jalkanen, R., Kirchhefer, A. & Robertson, I. (2019).

Cloud cover feedback moderates Fennoscandian summer temperature changes over the past 1000 years.

Geophysical Research Letters

<http://dx.doi.org/10.1029/2018GL081046>

This item is brought to you by Swansea University. Any person downloading material is agreeing to abide by the terms of the repository licence. Copies of full text items may be used or reproduced in any format or medium, without prior permission for personal research or study, educational or non-commercial purposes only. The copyright for any work remains with the original author unless otherwise specified. The full-text must not be sold in any format or medium without the formal permission of the copyright holder.

Permission for multiple reproductions should be obtained from the original author.

Authors are personally responsible for adhering to copyright and publisher restrictions when uploading content to the repository.

<http://www.swansea.ac.uk/library/researchsupport/ris-support/>

1 **Cloud cover feedback moderates Fennoscandian summer temperature changes over**
2 **the past 1000 years**
3

4 **Giles H.F. Young¹, Mary H. Gagen¹, Neil J. Loader¹, Danny McCarroll¹, Håkan Grudd²,**
5 **Risto Jalkanen³, Andreas Kirchhefer⁴ and Iain Robertson¹**
6

7 ¹ Geography Department, College of Science, Swansea University, Swansea, SA2 8PP, UK.

8 ² Swedish Polar Research Secretariat, SE-104 05 Stockholm, Sweden.

9 ³ Natural Resources Institute Finland, Metla, Eteläranta 55, 96300, Rovaniemi, Finland.

10 ⁴ Dendroøkologen, Skogåsvegen 6, NO-9011, Tromsø, Norway.
11

12 Corresponding author: Giles H.F. Young (g.h.f.young@swansea.ac.uk)
13

14 **Key Points:**

- 15 • Over recent decades, Northern Fennoscandian summer temperatures have increased little,
16 compared to those of the Northern Hemisphere.
- 17 • Cloud cover plays an important role in controlling temperature. Summers with more
18 cloud cover are cooler and those with less are warmer.
- 19 • During hemispheric warm periods, northern cloud cover increases, cooling regional
20 temperature, the opposite is true during cool periods.
21

22 **Abstract**

23 Northern Fennoscandia has experienced little summer warming over recent decades, in stark
24 contrast to the hemispheric trend, which is strongly linked to greenhouse gas emissions. A likely
25 explanation is the feedback between cloud cover and temperature. We establish the long- and
26 short-term relationship between summer cloud cover and temperature over Northern
27 Fennoscandia, by analysing meteorological and proxy climate data. We identify opposing
28 feedbacks operating at different timescales. At short timescales, dominated by internal
29 variability, the cloud cover-temperature feedback is negative; summers with increased cloud
30 cover are cooler and sunny summers are warmer. However, over longer timescales, at which
31 forced climate changes operate, this feedback is positive, rising temperatures causing increased
32 regional cloud cover and *vice versa*. This has occurred both during warm (Medieval Climate
33 Anomaly and at present) and cool (Little Ice Age) periods. This two-way feedback relationship
34 therefore moderates Northern Fennoscandian temperatures during both warm and cool
35 hemispheric periods.

36

37 **Plain Language Summary**

38 Temperatures have increased globally over recent decades, strongly linked to increases in
39 greenhouse gasses. However, over Northern Fennoscandia summer temperatures have increased
40 little over this period, although this region should be strongly affected by global warming. We
41 suggest that changes in summer cloud cover, driven by global temperature changes, are
42 responsible for this moderation of temperatures. This is happening now, and during past episodes
43 of climate change. We produce a new reconstruction of summer cloud cover for this region and
44 compare it to existing temperature reconstruction to establish the relationship between
45 temperature and cloud cover. We find that over short timescales, increased cloud cover leads to
46 cooler temperatures and *vice versa*. However, over longer timescales (decades to centuries) we
47 find that increased global temperature lead to increased northern cloud cover, which reduces
48 local temperatures (the medieval period and at present). The opposite being true in globally cool
49 periods, such as the Little Ice Age. These findings are important as they help to explain the
50 feedback relationship between cloud cover and temperature, which is one of the major
51 uncertainties in modelling future climate. Our data also confirm models of climate that suggest a
52 poleward movement of storm tracks during recent warming.

53 **1 Introduction**

54 Recent increases in global temperatures have been linked to the anthropogenic release of long-
55 lived greenhouse gases (IPCC, 2013). As these gases are well-mixed in the atmosphere, they
56 have a direct influence on the world-wide energy balance. However, at regional scales, feedbacks
57 operate amplifying or moderating temperature responses to global forcing, leading to regionally
58 enhanced or dampened changes. At high latitudes feedbacks tend to amplify the magnitude of
59 temperature response, and model projections suggest enhanced temperature increases over
60 regions such as Fennoscandia (IPCC, 2013). However, the instrumental records show that since
61 AD1859, summer (June-August) temperatures over northern Fennoscandia have increased little,
62 when compared to Northern Hemisphere trends (Osborn & Jones, 2014). A possible explanation
63 for the weaker regional response to hemispheric and global-scale forced warming is the
64 feedback relationship between temperature and cloud cover.

65 At present cloud cover, and especially low cloud cover, represents the single greatest uncertainty
66 in modelling future climate (Bony et al., 2006; Boucher et al., 2013). Both climate models and
67 observations suggest that with global warming there may be a poleward migration of the storm
68 tracks leading to higher levels of cloud cover in high-latitude regions such as Northern
69 Fennoscandia (Bender et al., 2012; Boucher et al., 2013; Norris et al., 2016). Clouds have an
70 important and complex feedback relationship with surface temperature (Boucher et al., 2013).
71 There is a negative feedback, reflecting shortwave radiation back into space, and a positive
72 feedback, retaining longwave radiation close to Earth's surface (Hartmann et al., 1992).
73 Resolving the feedback relationships between temperature and cloud cover is critical to
74 understanding past and future climatic change (Boucher et al., 2013)

75 Over short timescales, it is possible to define the feedback relationship using ground and satellite
76 data. Defining the relationship between temperature and cloud cover over the longer timescales,
77 at which both naturally and anthropogenically forced changes occur, is much more problematic
78 and requires reliable data for both variables. There is a strong history of reconstructing annual
79 summer temperature over Northern Fennoscandia (e.g. Esper et al., 2012; McCarroll et al., 2013)
80 and the Northern Hemisphere (e.g. D'Arrigo et al., 2006; Moberg et al., 2005; Shi et al., 2013;

81 Christiansen & Ljungqvist, 2012), and a number of robust millennial length reconstructions are
82 available.

83 It has become possible to produce reliable reconstructions of regional cloud cover, using stable
84 carbon isotopes ($\delta^{13}\text{C}$) from tree rings (Gagen et al., 2011a; Young et al., 2010; Helama et al.,
85 2018). The method works well using high latitude conifers, where carbon isotope fractionation is
86 dominated by photosynthetic rate rather than stomatal conductance, and therefore is mainly
87 controlled by photosynthetically active radiation (PAR) and linked strongly to the amount of
88 summer sunshine, and thus cloud cover. The relationship with cloud cover is therefore not direct
89 and is complicated by factors such as diffuse radiation being more effective for plant
90 photosynthesis. However, when a single, well replicated, measure of tree-ring $\delta^{13}\text{C}$ is compared
91 average summer sunshine or cloud cover, the relationship is strong and consistent through time
92 (Young et al., 2012; Loader et al., 2013). This methodological advance allows us to examine the
93 relationship between summer temperature and cloud cover over Northern Fennoscandia over the
94 last 1000 years. We combined millennial length, well replicated, $\delta^{13}\text{C}$ series from three locations
95 across northern Fennoscandia: Forfjord, Norway (Young et al., 2010; 2012); Torneträsk, Sweden
96 (Loader et al., 2013); and Laanila, Finland (Gagen et al., 2011a) (Figure S1), to produce a new
97 reconstruction of regional cloud cover. We use this new cloud cover reconstruction in
98 conjunction with regional temperature reconstructions and meteorological data for both cloud
99 cover and temperature to understand the complex and important relationship between cloud
100 cover and temperature over a millennial timescale.

101 **2 Methods**

102 2.1 Data

103 To determine the relationship between cloud cover and temperature over both long and short
104 timescales, we used both meteorological and proxy climate data.

105 2.1.1 Meteorological Data

106 2.1.1.1 Cloud Cover

107 Records of cloud cover for Northern Fennoscandia (c. N 65.0° to 70.0°, E 10.0° to 30.0°) are
108 available from ground and satellite data. A number of ground based series stretch back to the
109 nineteenth century (Tuomenvirta et al., 2001). Records of cloud cover measured by satellite,
110 since AD1983, are available from the International Satellite Cloud Climatology Project (ISCCP)
111 (Schiffer & Rossow, 1983). Ground and satellite cloud cover measurements match well over the
112 period of overlap (Figure S2).

113 2.1.1.2 Temperature

114 Long instrumental records are relatively abundant for this region and gridded data products, are
115 also available. We use the gridded data produced by the Climatic Research Unit (CRU), as they
116 clearly represent the grid boxes under analysis. The mean of the four equal area adjacent 5°x5°
117 boxes (centred on N 67.5°, E 12.5°; N 67.5°, E 17.5°; N 67.5°, E 22.5°; N 67.5°, E 27.5°) were
118 used to represent temperature of Northern Fennoscandia (Osborn & Jones, 2014; Jones et al.,
119 2007). We also use temperature records from the same four meteorological stations used to

120 derive our cloud cover composite (Figure S1), to compare directly the signal contained in tree
121 ring $\delta^{13}\text{C}$ for temperature and cloud cover. For hemispheric temperature, we also used data
122 produced from the CRU, CRUtemp4v Northern Hemisphere temperatures (Osborn & Jones,
123 2014).

124 To compare Northern Fennoscandian temperature to those of the Northern Hemisphere values
125 we scaled Northern Fennoscandian to those for the Northern Hemisphere over the period
126 AD1859-1980. Recent temperature increase was calculated by showing mean temperatures since
127 AD1981 as the difference from the AD1859–1980 mean.

128 2.1.2 Proxy Data

129 2.1.2.1 Isotopes

130 $\delta^{13}\text{C}$ measured from cellulose extracted from *Pinus sylvestris* L. tree rings, were used as a proxy
131 for summer cloud cover. Data from three locations (Forfjord, Torneträsk and Laanila (Figure
132 S1)) extending back over the past millennium were used (Young et al., 2010; 2012; Loader et al.,
133 2013; Gagen et al., 2011a).

134 2.1.2.2 Proxy Temperature Data

135 Two regional (Esper et al., 2012; McCarroll et al., 2013) and four hemispheric reconstructions
136 (D'Arrigo et al., 2006; Moberg et al., 2005; Shi et al., 2013; Christiansen & Ljungqvist, 2012)
137 of temperature were used to analyse the long term cloud cover-temperature relationship. To look
138 at periods of divergence between temperature and cloud cover, both series were z-scored over
139 the common period. $\delta^{13}\text{C}$ values were then subtracted from the temperature values to indicate
140 positive (cool/clear) and negative values (warm/cloudy) conditions. To compare regional and
141 hemispheric temperature reconstructions, individual series were z-scored over the common
142 period (AD1000–1973) and combined by taking the mean. This mean was then z-scored over the
143 same common period.

144 2.2 Combining Data

145 2.2.1 Cloud Cover and Temperature

146 Meteorological cloud cover and temperature composites (c. N 65.0° to 70.0°, E 10.0° to 30.0°)
147 were produced using data collected at four climate stations (Figure S1). The monthly values were
148 composited by taking the mean of the deviations from the climate normal period AD1961–1990.
149 This method has the dual advantages of, retaining the original units, while allowing the mean of
150 discontinuous data sets to be reliably established (Jones et al., 2012).

151 2.2.2 Isotopes

152 To produce a regional tree ring $\delta^{13}\text{C}$ chronology for the past millennium, we combined three
153 exiting, published, chronologies from northern Fennoscandia. These three millennial records of
154 tree-ring $\delta^{13}\text{C}$ were produced using slightly differing methodologies (Young et al., 2012; Loader
155 et al., 2013; Gagen et al., 2011a; 2011b). The Forfjord chronology was constructed entirely using
156 annual values from individual trees. Torneträsk was constructed using annual values from

157 individual trees, annually pooled values from multiple trees, and temporally pooled values from
158 individual trees (Loader et al., 2013). Laanila comprises temporally pooled values from
159 individual trees; while a shorter Laanila chronology stretching back to AD1652 (Gagen et al.
160 2007), comprises annual values from individual trees.

161 2.2.2.1 Annual Isotope Data

162 Annual data from the three locations are available for the period AD1652–2002 (Figure S1 and
163 S3), there is a significant match between the three series ($P < 0.001$). The series were z-scored and
164 the mean was taken to produce an annual series from AD1652–2002. This mean, over the period
165 AD1890–2002, was used for calibration purposes.

166 2.2.2.2 Non-Annual Isotope Data

167 Prior to AD1652 no annualised data are available for the Laanila site, while both the Forfjord and
168 Torneträsk are comprised of annually resolved values. Combining the three isotope series
169 involved four steps. Firstly, the Forfjord and Torneträsk series were degraded to the same
170 temporal resolution as the Laanila series, by treating each series with a 9-year Gaussian filter.
171 Secondly, the annualised series from Forfjord and Torneträsk were subtracted from their
172 respective filtered series and averaged, to create a high frequency data set. Thirdly, a mean was
173 taken of the Laanila and the filtered Forfjord and Torneträsk series to create a low frequency
174 composite. Fourthly, the high frequency series created in step two was added to the low
175 frequency series created in step four, producing a composite series combining low frequency
176 data from Laanila, Forfjord and Torneträsk and the high frequency data from Forfjord and
177 Torneträsk (Figure S4).

178 2.3 Calibration

179 Climate calibration was carried out using standard methods for annual proxy data (NRC, 2006).
180 Both the proxy and climate data were divided into two parts (AD2002–1946 and AD1945–1890).
181 Calibration was undertaken over each periods, and then verified using the other period. Three
182 statistics were calculated for each pair of calibrations and verifications: the squared correlation
183 coefficient (R^2); the reduction of error (RE); and the coefficient of efficiency (CE).

184 2.4 Reconstruction

185 Reduced major axis regression (RMA), often referred to as variance scaling, was used to
186 reconstruct cloud cover from the $\delta^{13}\text{C}$ data. The method scales the proxy to the mean and
187 variability of the climate target over the instrumental period, giving a more realistic
188 reconstruction of climate variability than ordinary least squares (OLS) regression.

189 2.5 Scaling versus Regression and Extreme Value Capture Tests

190 A problem with RMA regression is that there is an inevitable increase in error compared to an
191 OLS reconstruction, as the increase in variance inevitably increase the error (McCarroll et al.,
192 2015). If the proxy relationship with climate is not sufficiently strong, the result will be a
193 reconstruction which is scaling noise, rather than signal and the predictive skill of the
194 reconstruction will fall below zero. A simple metric, R^2_{vs} (R^2 variance scaled), was proposed to

195 determine this (McCarroll et al., 2015). When the correlation between proxy and climate falls
196 below $r = 0.5$, R^2_{vs} will fall below zero, the predictive skill of the reconstruction will be less than
197 that of the mean climatology over the calibration period.

198 An extreme value capture (EVC) test (McCarroll et al., 2015) is used to establish whether the
199 correct values are being pushed to the extreme by RMA regression. The test determines whether
200 the increase in error, inevitable when scaling, is sufficiently counterbalanced by a more effective
201 expression of the extreme values.

202 2.6 Uncertainties

203 A typical approach is to use two standard errors (2SE) of the prediction (c. 95% confidence
204 interval). However, this does not quantify uncertainty relating to changes in sample depth and
205 coherence prior to the instrumental period. Adding a measure of uncertainty based upon series
206 coherence goes some way towards resolving this problem; but if this figure merely added to the
207 2SE it will tend to exaggerate uncertainty (McCarroll et al., 2013), as the 2SE of the calibration
208 also encompasses an element of this uncertainty. We therefore use the 2SE of the regression
209 equation as a base error throughout the reconstruction, adding to this the 95% confidence interval
210 of the coherence between the three series, in units of cloud cover, where and by the amount it
211 exceeds 2SE (Figure S5).

212 3 Results

213 3.1 Meteorological temperature

214 Data, calculated using regional gridded temperature and hemispheric temperatures (Osborn &
215 Jones, 2014), shows that while mean annual and summer Northern Hemispheric temperatures
216 have increased considerably since records began, the increase of mean annual and especially
217 mean summer Northern Fennoscandia temperature has been very modest. Northern
218 Fennoscandia summer temperature rise since AD1859 is only 14.05% of that of the Northern
219 Hemisphere mean (Figure 1), while the annual increase is less than a third (25.8%).

220

221 3.2 Meteorological temperature and cloud cover

222 Summer monthly mean cloud cover has a strongly negative relationship with summer mean
223 temperature ($r = -0.80$, $P < 0.001$), explaining 64% of the variability in summer temperature
224 variability (Figure S6). Therefore, during the summer months (June–August), when skies are
225 clear, summers are warm and when cloud cover increases summers become cooler. When
226 estimated by linear trend there has been an increase of 4.5% in observed summer cloud cover
227 over the twentieth century ($r = 0.2$, $P < 0.5$). Temperature over the same period has increased but
228 by only c. 1°C , and since AD1930 — in marked contrast to the hemispheric trend — temperature
229 has not increased at all (linear trend -0.5°C). From the available meteorological, satellite and
230 model simulation data (Bony et al., 2006; Norris et al., 2016), there is also evidence that cloud
231 cover over Fennoscandia may have increased with hemispheric temperature.

232 3.3 Isotopic cloud cover calibration and reconstruction

233 The correlation between observed summer cloud cover and the $\delta^{13}\text{C}$ composite is strong ($r =$
234 0.75 , $P < 0.001$), and passes verification tests for climate reconstructions (Table S1 and Figure 2A
235 & B). When temperature data from the same climate stations are used the relationship with $\delta^{13}\text{C}$
236 is still significant ($r = 0.58$, $P < 0.001$), but considerably weaker and the relationship only passes
237 the RE verification, failing the important CE test (Figure S7). The data $\delta^{13}\text{C}$ are therefore much
238 more suitable for a palaeoclimatic reconstruction of past cloud cover variability than
239 temperature. The relationship between cloud cover and our $\delta^{13}\text{C}$ composite is considerably
240 higher than the threshold of $r = 0.5$, established by McCarroll et al. (2015) for RMA (scaling).
241 The scaled data also much more efficient at capturing extreme values (12 out of 24) in the
242 meteorological data, than regression (6 out of 24) (Figure S8). We therefore produced a
243 reconstruction of summer cloud cover over Northern Fennoscandia from AD990-2002 using
244 RMA regression (Figure 2A). The reconstruction shows considerable variability in cloud cover
245 over the past 1000-years with a maximum in AD1017 ($+12.98\% \pm 7.43$) and a minimum in
246 AD1698 ($-19.31\% \pm 9.20$). The decade with the highest cloud cover was the AD1490s ($+3.35\%$
247 ± 7.43) and the sunniest decade was the AD1750s ($-9.30\% \pm 7.88$). There were notable extended
248 periods of high cloud cover in the 11th century, the 14th and 15th centuries, and the 20th century.
249 There was a lengthy extended sunny period from AD1550 to AD1800. Our reconstruction also
250 clearly shows that most of the past 1000 years has been sunnier than recent decades. All but one
251 (AD1450) of the 10 sunniest years and calendar decades (AD1291–1300) and all of the sunniest
252 30-year periods, fall within the prolonged period of reduced cloud cover between c. AD1550 and
253 1800, which corresponds with the European Little Ice Age.

254 To analyse the long-term (millennial) relationship between temperature and cloud cover we
255 compared our $\delta^{13}\text{C}$ composite with published records of temperature from proxy sources for both
256 Northern Fennoscandia and the Northern Hemisphere. When compared with hemispheric
257 reconstructions, used in the latest IPCC report (D'Arrigo et al., 2006; Moberg et al., 2005; Shi et
258 al., 2013; Christiansen & Ljungqvist, 2012) our proxy record of cloud cover shows clear periods
259 of divergence (Figures 3 & S9). During three extended periods: AD990–1125, the latter stages of
260 the Medieval Climate Anomaly (MCA); AD1575-1850, Little Ice Age (LIA); and since AD1900,
261 there are large directional changes in Northern Fennoscandian cloud cover, in response to forced
262 hemispheric temperature changes. This palaeoclimatic perspective shows that at multi-decadal
263 and centennial timescales there is an anti-phase between summer temperature and the $\delta^{13}\text{C}$
264 composite, a positive relationship between hemispheric temperatures and Fennoscandian cloud
265 cover. Therefore, the opposite of that observed from meteorological records (Section 3.1).

266 3.4 Comparison of reconstructed hemispheric and Northern Fennoscandian temperature

267 We also compared the temperature over Northern Fennoscandia with that of the Northern
268 Hemisphere over the past millennium (Figure S10). This comparison shows that, while
269 reconstructed temperatures trends over the past 1000 years follow a generally similar pattern,
270 with warmer than average temperatures in the medieval period and at present, the magnitude of
271 the changes is muted over Northern Fennoscandia. Indeed, there is little sign of the prolonged
272 cool period between c. AD1525 and AD1850 often referred to as the LIA.

273 4 Discussion

274 The feedback relationship between cloud cover and temperature is extremely important over
275 northern Fennoscandia as can be seen in Figure S6. In winter, it is positive, with low-level cloud
276 cover acting to retain heat at the surface. However, during the growing season, the cloud cover-
277 temperature relationship is a strongly negative one. Higher percentages of cloud cover lead to
278 reduced summer temperatures and lower percentages increased temperatures. Cloud cover,
279 therefore, plays an extremely important role in moderating surface temperature over northern
280 Fennoscandia, especially during summer months.

281 In contrast, palaeoclimatic data clearly show that the long-term relationship between summer
282 temperature and cloud cover is a positive one, in the opposite direction to that which operates
283 over shorter timescales. During hemispheric periods of prolonged warmth (the medieval and at
284 present) summer cloud cover increases, and during cool periods (c. AD1525-1850) summer cloud
285 cover decreases. There are two possible explanations for this. Firstly, that during warm periods
286 there is an increase in northern cloud cover, due to a northerly drift in the storm tracks. This
287 hypothesis fits model projections and short-term studies from satellite data (Norris et al., 2016),
288 which predict a poleward movement of the mid-latitude storm tracks in direct response to forced
289 global warming, and by inference the opposite during cooler periods. Secondly, that during
290 warm/cool periods the atmosphere has a lower/higher water holding capacity, which leads to
291 higher/lower cloud cover. These two hypotheses are, of course, not mutually exclusive and can
292 clearly operate at the same time. However, second hypothesis appears less likely than the first, as
293 it is clear from the meteorological data that as there is not a significant increase in cloud cover
294 during warm summers and also the position of the region means that it receives much of its
295 precipitation from Atlantic frontal systems.

296 Our results suggest that over Northern Fennoscandia, there may be a complex two-way
297 relationship between surface temperature and cloud cover. The cloud cover-temperature
298 feedback appears to operating in opposing directions over different timescales (Figure 4). Over
299 short timescales, cloud cover imposes a negative feedback on regional temperature; cloudy
300 summers with increased cloud are on average cooler and summers with less cloud cover are
301 warmer. This relationship is clear from the meteorological records (Figure S6). Our data suggest
302 however, that over longer time-scales, hemispheric temperature changes lead to directional
303 changes in regional cloud cover (Figure 3). Over these time-scales, the feedback relationship
304 appears to be a positive one: warm periods have increased cloud cover and cool periods less
305 cloud cover (Figure 4). Over recent decades, anthropogenically forced global temperature rises
306 appear to have led to an increase in regional cloud cover (Bender et al., 2012; Boucher et al.,
307 2013; Norris et al., 2016). Our data suggest that such an increase in cloud cover should have a
308 negative feedback effect on regional summer temperature (Figure S6), resulting in a muted
309 temperature increase, relative to the rest of the hemisphere (Figure 1). The same dampening of
310 regional temperatures can also be seen in the palaeoclimatic record (Figures S10). During the
311 hemispherically warm Medieval (prior to c. AD1100), and cool LIA, c. AD1550–1850 (Matthews
312 and Briffa, 2005) periods, directional changes in summer cloud cover have acted to moderate the
313 degree of regional summer warming and cooling.

314 Our model (Figure 4) predicts that summer surface temperature changes over Northern
315 Fennoscandia are moderated by the associated change in cloud cover. This can be tested by
316 looking at both the meteorological and the palaeo data. Figure 1 clearly shows that summer
317 temperatures over Northern Fennoscandia have risen very modestly when compared to Northern

318 Hemisphere changes. While Figure S10 places this clearly into the context of large-scale, long-
319 term, forced climate change of the past millennium, showing that Northern Fennoscandian
320 temperatures show lower long-term variability than Northern Hemisphere temperatures,
321 especially in key periods of forced climate change the MCA, the LIA and the late twentieth
322 century.

323 **5 Conclusions**

324 Measures of tree growth, including ring widths and maximum densities, provide some of the
325 most powerful methods for reconstructing past summer temperatures at annual resolution over
326 long timescales. Our results suggest that they can now be combined with stable carbon isotope
327 ratios from suitable tree rings to produce parallel records of changes in summer sunshine and/or
328 cloud cover, providing unique insights into the long-term relationship between cloud cover and
329 temperature, which remains the greatest source of uncertainty in modelling the climate of the
330 future.

331 While Northern Hemispheric temperature has shown substantial average increases over recent
332 decades, the temperature of Northern Fennoscandia has remained fairly static. This can be linked
333 to changes in summer cloud cover, especially when considered in the longer palaeoclimatic
334 context. Over the past 1000-years as forced hemispheric temperatures have increased/decreased
335 regional cloud cover has increased/decreased; leading to a moderating effect on regional
336 temperatures.

337 Our observations, based on palaeoclimatic proxies, confirm what has been suggested by climatic
338 models, that increasing global temperature leads to increased cloud cover at high-latitudes. Our
339 data also suggest that this is a two-way process, with warm conditions leading to increased cloud
340 cover and cool conditions reduced cloud cover.

341 **Acknowledgments and Data**

342 This research was funded by the EU funded Millennium Project (017008) and was made possible
343 by discussions with many of the collaboration scientists. GHFY, NJL and DM also acknowledge
344 support from The Leverhulme Trust (RPG-2014-327) and NERC (NE/P011527/1).

345 The proxy data sets required to produce this research are archived on the NOAA
346 Paleoclimatology Data Base at [https://www.ncdc.noaa.gov/data-access/paleoclimatology-](https://www.ncdc.noaa.gov/data-access/paleoclimatology-data/datasets)
347 [data/datasets](https://www.ncdc.noaa.gov/data-access/paleoclimatology-data/datasets). Climate data are available from the Climatic Research Unit at the University of
348 East Anglia <http://www.cru.uea.ac.uk/data> and The Royal Netherlands Meteorological Institute
349 (KNMI) Climate Explorer <https://climexp.knmi.nl>.

350 **References**

351 Bender, F. A.-M., Ramanathan, V., & Tselioudis, G. (2012), Changes in extratropical storm track
352 cloudiness 1983–2008: observational support for a poleward shift, *Clim. Dynam.*, 38, 2037-
353 2053, doi:10.1007/s00382-00011-01065-00386.

354

355 Bony, S., Colman, R., Kattsov, V. M., Allan, R. P., Bretherton, C. S., Dufresne, J.-L., et al.
356 (2006), How well do we understand and evaluate climate change feedback processes?, *J. Clim.*,
357 19, 3445-3482.
358

359 Boucher, O., Randall, D., Artaxo, P., Bretherton, C., Feingold, G., Forster, P., et al. (2013),
360 Clouds and Aerosols, in *Climate Change 2013: The Physical Science Basis. Contribution of*
361 *Working Group I to the Fifth Assessment Report of the Intergovernmental Panel on Climate*
362 *Change*, edited by Stocker, T. F., Qin, D., Plattner, G.-K., Tignor, M., Allen, S. K., Boschung, J.,
363 et al., pp. 571-657, Cambridge University Press, Cambridge, United Kingdom.
364

365 Christiansen, B., & Ljungqvist, F. C. (2012), The extra-tropical Northern Hemisphere
366 temperature in the last two millennia: reconstructions of low-frequency variability, *Clim. Past*, 8,
367 765–786, doi:710.5194/cp-5198-5765-2012.
368

369 D'Arrigo, R. D., Wilson, R., & Jacoby, G. C. (2006), On the long-term context for late twentieth
370 century warming, *J. Geophys. Res.*, 111(D3), doi:10.1029/2005JD006352.
371

372 Esper, J., Frank, D., Timonen, M., Zorita, E., Wilson, R. J. S., Luterbacher, J., et al. (2012),
373 Orbital forcing of tree-ring data, *Nat. Clim. Change*, 2, 862-866, DOI:810.1038/nclimate1589.
374 Gagen, M., McCarroll, D., Jalkanen, R., Loader, N. J., Robertson, I., & Young, G. H. F. (2011),
375 A rapid method for the production of robust millennial length stable isotope tree ring series for
376 climate reconstruction, *Glob. Planet. Chang.*, doi:10.1016/j.gloplacha.2011.1011.1006.
377

378 Gagen, M. H., McCarroll, D., Loader, N. J., Robertson, I., Jalkanen, R., & Anchukaitis, K. J.
379 (2007), Exorcising the 'segment length curse': summer temperature reconstruction since AD
380 1640 using non-detrended stable carbon isotope ratios from pine trees in northern Finland,
381 *Holocene*, 17(4), 435-446.
382

383 Gagen, M. H., McCarroll, D., Jalkanen, R., Loader, N. J., Robertson, I., & Young, G. H. F.
384 (2011a), A rapid method for the production of robust millennial length stable isotope tree ring
385 series for climate reconstruction, *Glob. Planet. Chang.*, doi:10.1016/j.gloplacha.2011.1011.1006.
386

387 Gagen, M. H., Zorita, E., McCarroll, D., Young, G. H. F., Grudd, H., Jalkanen, R., et al. (2011b),
388 Cloud response to summer temperatures in Fennoscandia over the last thousand years., *Geophys.*
389 *Res. Lett.*, 38, L05701, doi:05710.01029/02010GL046216.
390

391 Hartmann, D. L., Ockert-Bell, M. E., & Michelsen, M. L. (1992), The effect of cloud type on
392 earth's energy balance: global analysis, *J. Clim.*, 5, 1281-1304.
393

394 Helama, S., Arppe, L., Timonen, M., Mielikäinen, K., & Oinonen, M. (2018), A 7.5 ka
395 chronology of stable carbon isotopes from tree rings with implications for thier use in palaeo-
396 cloud reconstruction, *Glob. Planet. Chang.*, 170, 20-33.
397

398 IPCC (2013), *Climate Change 2013: The Physical Science Basis. Working Group I Contribution*
399 *to the Fifth Assessment Report of the Intergovernmental Panel on Climate Change*, Cambridge
400 University Press, Cambridge.

401
402 Jones, P. D., Lister, D. H., Osborn, T. J., Harpham, C., Salmon, M., & Morice, C. P. (2012),
403 Hemispheric and large-scale land-surface air temperature variations: An extensive revision and
404 an update to 2010, *J. Geophys. Res.*, 117, D05127, DOI 05110.01029/02011JD017139.
405
406 Loader, N. J., Young, G. H. F., Grudd, H., & McCarroll, D. (2013), Stable carbon isotopes from
407 Torneträsk, northern Sweden provide a millennial length reconstruction of summer sunshine and
408 its relationship to Arctic circulation, *Quaternary Sci. Rev.*, 62, 97-113.
409
410 Matthews, J. A., & Briffa, K. R. (2005), The 'Little Ice Age': a re-evaluation of an evolving
411 concept, *Geogr. Ann. A*, 87A, 17-36.
412
413 McCarroll, D., Young, G. H. F., & Loader, N. J. (2015), Measuring the skill of variance-scaled
414 climate reconstructions and a test for the capture of extremes, *Holocene*, 25(4), 618-626, doi:
415 610.1177/0959683614565956.
416
417 McCarroll, D., Loader, N. J., Jalkanen, R., Gagen, M., Grudd, H., Gunnarson, B. E., et al.
418 (2013), A 1200-year multi-proxy record of tree growth and summer temperature at the northern
419 pine forest limit of Europe, *Holocene*, 23(4), 471-484, doi:410.177/0959683612467483.
420 Moberg, A., Sonechkin, D. M., Holmgren, K., Datsenko, N. M., & Karlén, W. (2005), Highly
421 variable Northern Hemisphere temperatures reconstructed from low- and high-resolution proxy
422 data, *Nature*, 433, 613-617.
423
424 Norris, J. R., Allen, R. J., Evan, A. T., Zelinka, M. D., O'Dell, C. W., & Klein, S. A. (2016),
425 Evidence for climate change in the satellite cloud record, *Nature*, 536, 72-75,
426 doi:10.1038/nature18273.
427
428 NRC (2006), *Surface Temperature Reconstructions for the Last 2,000 Years*, The National
429 Academies, Washington, D.C.
430
431 Osborn, T. J., & Jones, P. D. (2014), The CRUTEM4 land-surface air temperature data set:
432 construction, previous versions and dissemination via Google Earth, *Earth Syst. Sci. Data*, 6, 61-
433 68, DOI 10.5194/essd-5196-5161-2014.
434
435 Schiffer, R. A., & Rossow, W. B. (1983), The International Satellite Cloud Climatology Project
436 (ISCCP): The First Project of the World Climate Research Programme, *Bull. Am. Meteorol.*
437 *Soc.*, 64, 779-784.
438
439 Shi, F., Yang, B., Mairesse, A., von Gunten, L., Li, J., Bräuning, A., et al. (2013), Northern
440 Hemisphere temperature reconstruction during the last millennium using multiple annual
441 proxies, *Climate Research*, 56, 231-244, doi:210.3354/cr01156.
442
443 Tuomenvirta, H., Drebs, A., Førland, E., Tveito, O. E., Alexandersson, H., Laursen, E. V., &
444 Jónsson, T. (2001), *Nordklim data set 1.0 - description and illustrations Rep.*, Report 08/01.
445 Norwegian Meteorological Institute, Oslo.
446

447 Young, G. H. F., McCarroll, D., Loader, N. J., & Kirchhefer, A. J. (2010), A 500-year record of
448 summer near-ground solar radiation from tree-ring stable carbon isotopes, *Holocene*, 20(3), 315-
449 324, doi: 310.1177/0959683609351902.

450
451 Young, G. H. F., McCarroll, D., Loader, N. J., Gagen, M., Kirchhefer, A. J., & Demmler, J. C.
452 (2012), Changes in atmospheric circulation and the Arctic Oscillation preserved within a
453 millennial length reconstruction of summer cloud cover from northern Fennoscandia, *Clim.*
454 *Dynam.*, 39, 495-507, doi:410.1007/s00382-00011-01246-00383.

455
456
457
458
459
460

461 **Figure Captions**

462

463 **Figure 1.** Comparison of CRUtemp4v (Osborn & Jones, 2014) Northern Hemisphere (NH, blue)
464 and Northern Fennoscandian temperature (NF, red) annual and summer (June-August) means,
465 over the common period AD1859-2017. NF values have been scaled to those for the NH over the
466 period AD1859-1980 for comparison. Recent temperature increase was calculated by showing
467 mean NH and NF temperature since AD1981 as the difference from the AD1859–1980 mean. The
468 percentage of NF to the NH temperature increase, over the period since AD1981 are also shown in
469 the adjacent bar graphs.

470

471 **Figure 2.** (A) Percentage of summer cloud cover (as deviations from the AD1961-1990 mean)
472 reconstructed from $\delta^{13}\text{C}$ composite (grey line) for the period AD990–2002, observed cloud cover
473 AD1890–2002 (red line). The reconstruction was made using reduced major axis regression
474 (variance scaling). (B) Scatter-graph for the squared correlation coefficient between observed
475 summer cloud cover and reconstructed cloud cover. (C) Observed (red line) and reconstructed
476 cloud (grey line) over the period for which meteorological cloud cover and the reconstruction
477 overlap (AD1890–2002).

478

479 **Figure 3.** To indicate periods of divergence between temperature and cloud cover, the z-scored
480 stable carbon isotope chronology were subtracted from the z-scored NH temperature
481 reconstructions (Moberg et al., 2005; Shi et al., 2013). Positive values indicate cool/clear and
482 negative values warm/cloudy conditions.

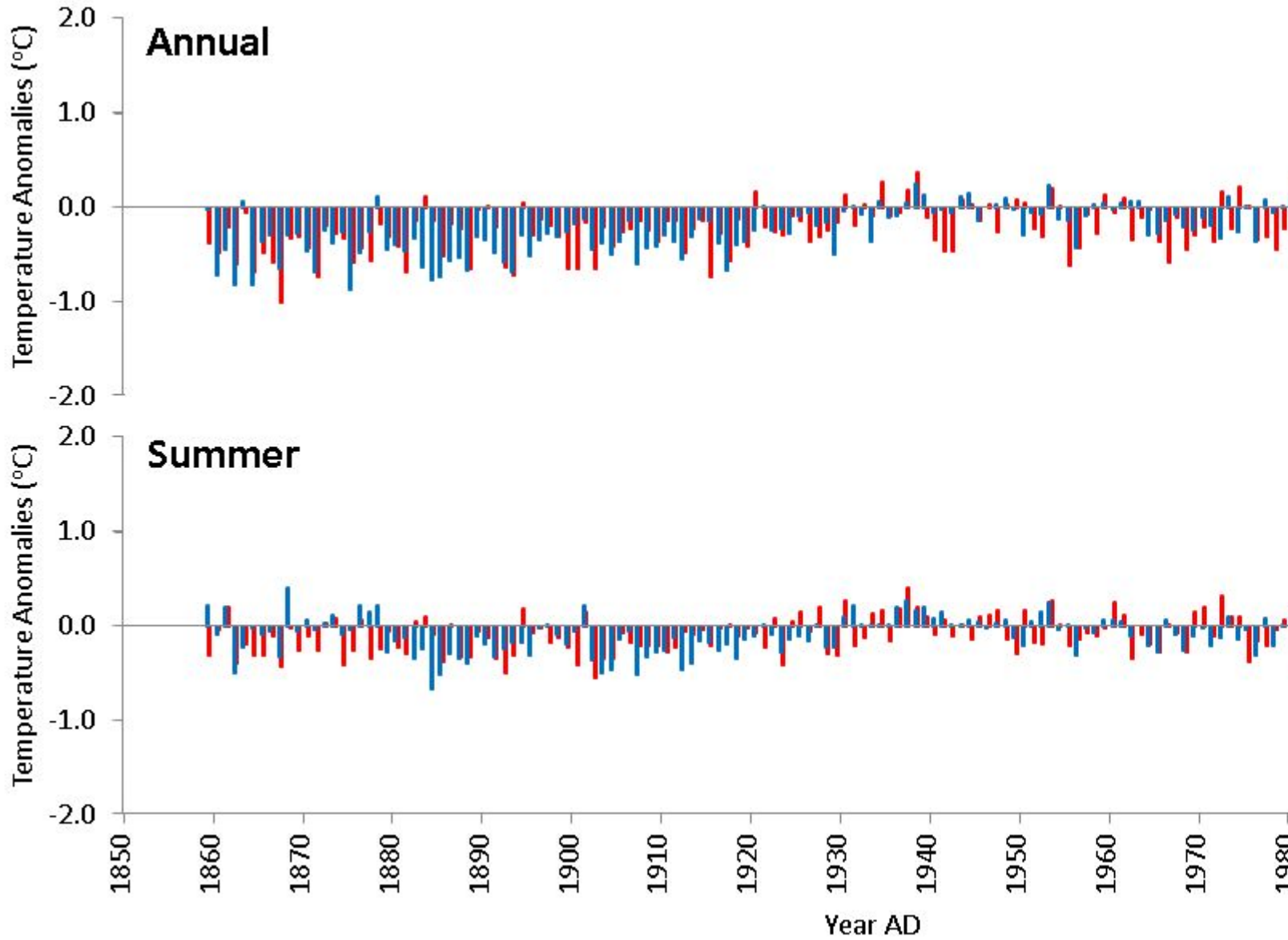
483

484 **Figure 4.** The feedback relationship between temperature and cloud cover over short (unforced)
485 and longer (forced) timescales. Over short timescales increased cloud cover reduces summer
486 temperature. Over longer timescales increased temperatures result in a reorganisation of
487 circulation and an increase in Northern Fennoscandian cloud cover.

488

Figure 1.

Annual



Summer

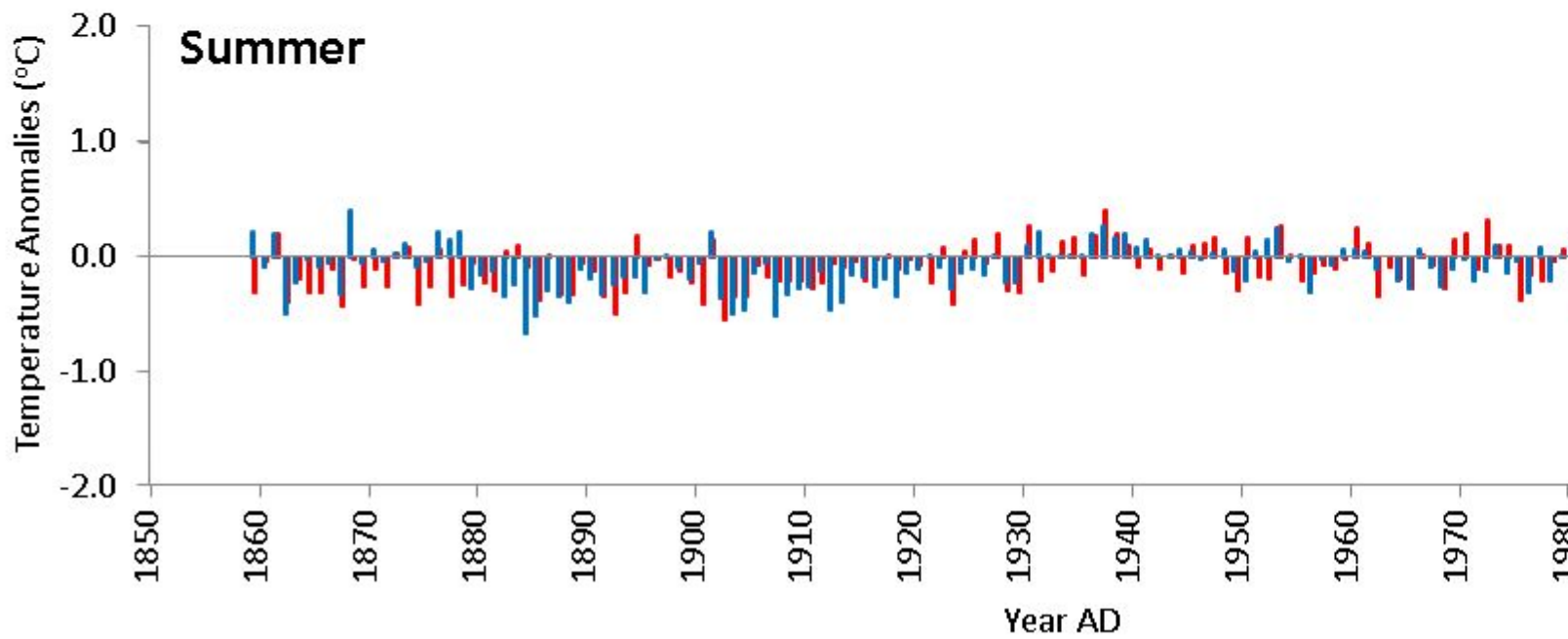


Figure 2.

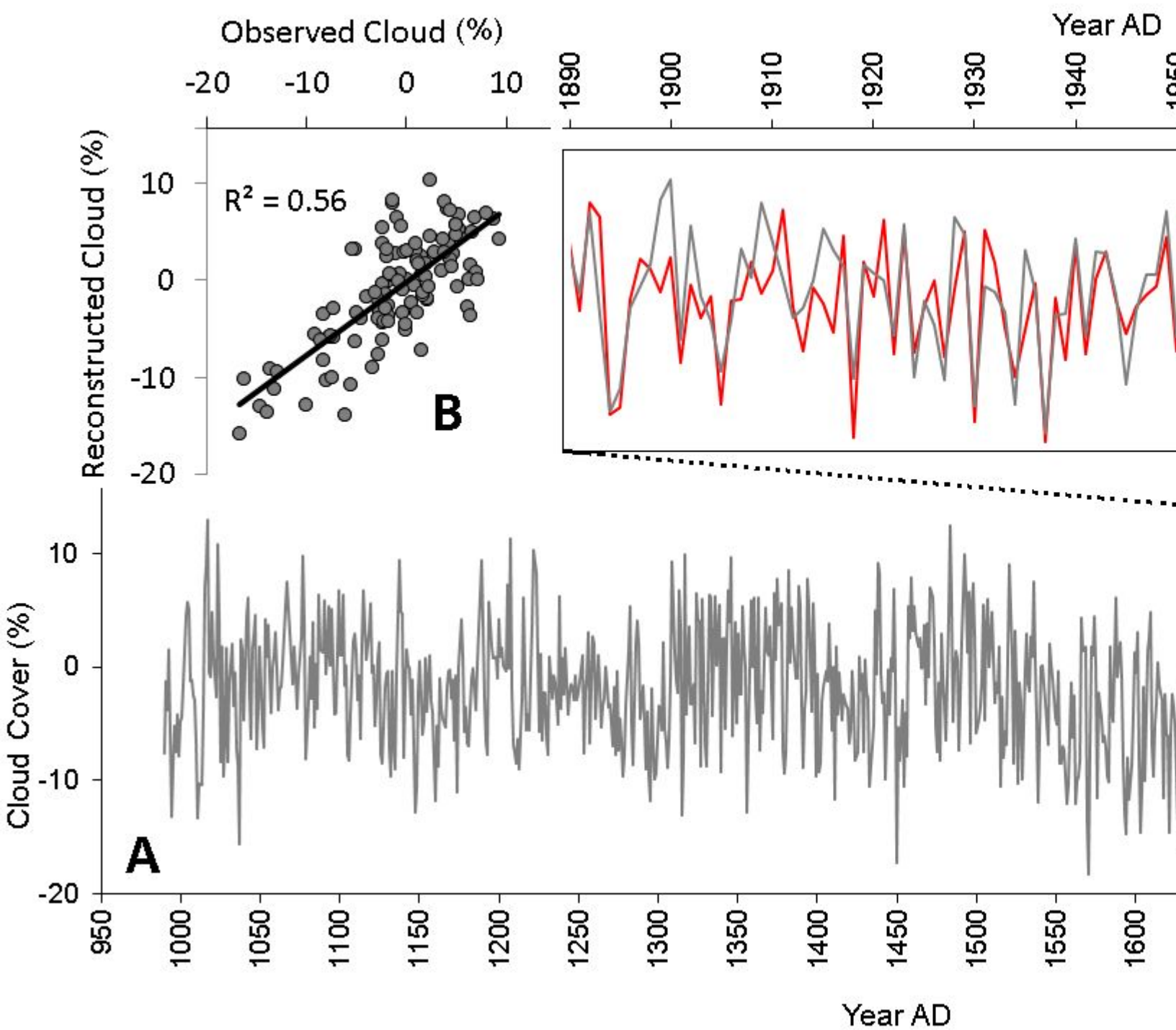


Figure 3.

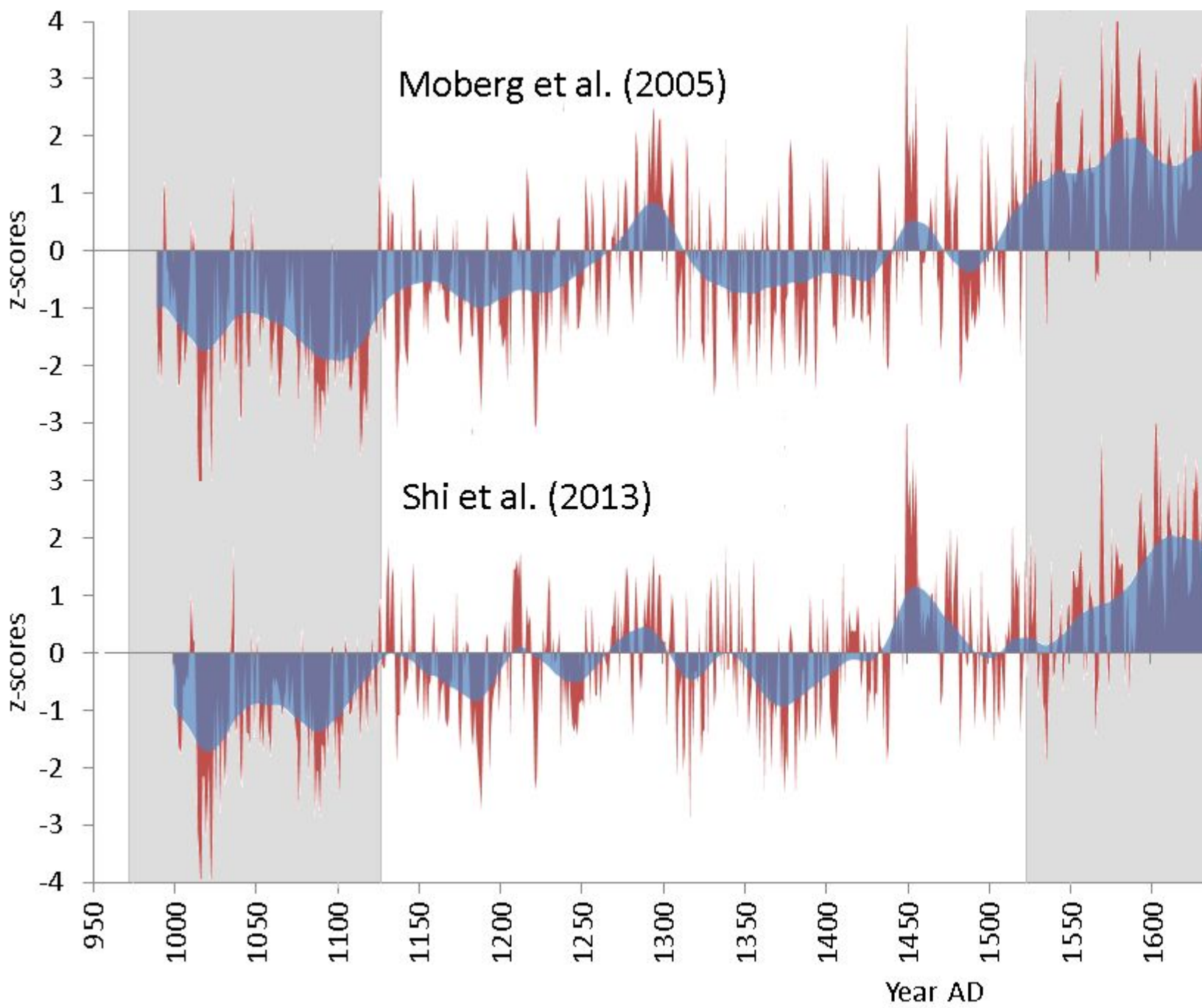


Figure 4.

Short time-scales,
Internal variability



Negative -

Cloud cover

Temperature

Positive +



Long time-scales,
Forced changes